

Retraction

Retracted: Prediction of Long-term Variation of Ocean Circulation Based on Grey Correlation Clustering

Mobile Information Systems

Received 26 September 2023; Accepted 26 September 2023; Published 27 September 2023

Copyright © 2023 Mobile Information Systems. This is an open access article distributed under the Creative Commons Attribution License, which permits unrestricted use, distribution, and reproduction in any medium, provided the original work is properly cited.

This article has been retracted by Hindawi following an investigation undertaken by the publisher [1]. This investigation has uncovered evidence of one or more of the following indicators of systematic manipulation of the publication process:

- (1) Discrepancies in scope
- (2) Discrepancies in the description of the research reported
- (3) Discrepancies between the availability of data and the research described
- (4) Inappropriate citations
- (5) Incoherent, meaningless and/or irrelevant content included in the article
- (6) Peer-review manipulation

The presence of these indicators undermines our confidence in the integrity of the article's content and we cannot, therefore, vouch for its reliability. Please note that this notice is intended solely to alert readers that the content of this article is unreliable. We have not investigated whether authors were aware of or involved in the systematic manipulation of the publication process.

Wiley and Hindawi regrets that the usual quality checks did not identify these issues before publication and have since put additional measures in place to safeguard research integrity.

We wish to credit our own Research Integrity and Research Publishing teams and anonymous and named external researchers and research integrity experts for contributing to this investigation.

The corresponding author, as the representative of all authors, has been given the opportunity to register their agreement or disagreement to this retraction. We have kept a record of any response received.

References

- [1] N. Ma and G. Yang, "Prediction of Long-term Variation of Ocean Circulation Based on Grey Correlation Clustering," *Mobile Information Systems*, vol. 2022, Article ID 4791054, 8 pages, 2022.

Research Article

Prediction of Long-term Variation of Ocean Circulation Based on Grey Correlation Clustering

Na Ma ¹ and Guoshu Yang²

¹Gaomi College, Qingdao University of Science and Technology, Qingdao, Shandong 261500, China

²School of Mathematics and Physics, Qingdao University of Science and Technology, Qingdao, Shandong 261500, China

Correspondence should be addressed to Na Ma; 20181111121718@stu.hubu.edu.cn

Received 24 June 2022; Revised 11 September 2022; Accepted 17 September 2022; Published 30 September 2022

Academic Editor: Xuefeng Zhang

Copyright © 2022 Na Ma and Guoshu Yang. This is an open access article distributed under the Creative Commons Attribution License, which permits unrestricted use, distribution, and reproduction in any medium, provided the original work is properly cited.

In order to study the change of circulation in the South China Sea, the author puts forward the research on the distribution and change of water masses in the South China Sea based on grey correlation clustering. Based on the wod21 temperature and salt observation data of the South China Sea from 1966 to 2013, this paper uses the grey correlation clustering algorithm to divide the water masses in the whole sea area and $5^\circ \times 5^\circ$ small areas and analyzes the distribution, temperature, salt properties, and seasonal changes of each water mass in the South China Sea combined with the systematic clustering method and T-S point clustering map. The experimental results show that in the vertical division, the South China Sea water mass is divided into five layers: surface water, subsurface water, sub-middle water, middle water, and deep water. The deep water in the South China Sea is mainly distributed in the basin with a depth of 900 m. The temperature value is lower than 5.5°C and the salinity range is 34.30–34.70. The properties and changes of water masses obtained in this paper are consistent with the existing conclusions, which shows that the grey correlation clustering algorithm is efficient and accurate in the division of water masses in the South China Sea.

1. Introduction

An accurate assessment of global ocean circulation change is a key in understanding the change of Earth's climate system and predict its future change trend [1]. For a long time, there is a basic scientific question that people urgently want to answer in terms of ocean circulation and climate "how does Earth's ocean circulation system change under the background of global warming?" However, there are great difficulties in answering this question. On the one hand, the changes in Earth's ocean circulation are very regional and complex. Under the forcing of greenhouse gas emissions, there are significant differences in the response of ocean circulation in different regions to climate change, as shown in Figure 1. For example, the subtropical western boundary current, the Pacific wind-driven circulation, and the Indonesian through current have a strengthening trend, which leads to rapid warming in relevant regions. The Angoras current has not accelerated since the 1990s, while the

Atlantic meridional overturning circulation shows a slowing trend [2]. These regional differences are mainly caused by the dynamic process adjustment within the climate system. The dynamic adjustment of ocean circulation in different regions is very different, resulting in great differences in the estimation of its multidecadal trend. On the other hand, human beings still lack systematic and continuous direct observation of Earth's ocean circulation [3]. Historically, most of the observations of global ocean circulation have focused on some specific domains and time periods. The regional differences in ocean circulation make it difficult to monitor the overall changes of Earth's general circulation system with these specific observations.

2. Literature Review

Dias and others first used the equation of seawater motion to study the problem of ocean currents, trying to explain the cause of ocean currents with wind stress. However, they did



- The monsoon
- Intra-seasonal oscillation
- The typhoon
- El nino

FIGURE 1: Variation of ocean circulation.

not understand the disaster state motion of seawater at that time and did not understand the significance of disaster in the momentum exchange of seawater, so they dealt with this problem with the molecular viscosity of seawater. Therefore, an unreasonable result is obtained: the wind stress needs to act continuously for thousands of years to form a stable ocean current. At the same time, the impact of Earth's rotation on ocean currents has not been understood in the study [4]. Scheen and others first recognized the important role of geostrophic deflection force (Coriolis force) in wind-driven ocean currents [5]; Liu and others derived a formula for calculating the current velocity using the slope of the isobaric surface. However, these two research results were not valued by oceanographers at that time [6]. Raj and others put forward the famous "wind ocean current theory". On the premise of considering the effect of Coriolis force on an ocean current, the velocity field of wind ocean current in the friction layer on the sea surface is successfully calculated for the first time according to the sea surface wind stress. The establishment of "circulation theory" and "wind ocean current theory" has made the research of ocean circulation have a solid mathematical theoretical foundation and began to use the motion equation to study the average motion of seawater [7]. Hao and others proposed the important role of inertial effect in the formation of current bending, but he applied the simplified disturbance equation, so it is still linear [8]. Sobisevich and others have played a direct role in promoting the study of nonlinear current theory [9]. On this basis, Zhao and others calculated the flow and velocity of the cross flow and the width of the Gulf Stream according to the principle of conservation of potential hazard degree, which is in good agreement with the measured results [10]. These nonlinear theories do not include any accidental parameters, which is also an advantage over the full flow theory. However, due to the complexity of mathematical processing of nonlinear problems, there are still some difficulties in the research of this theory in the 1990s when computer technology has not yet sprung up. With the rapid development of

computer technology, the research of nonlinear theory has been greatly developed. Scholars can use the computer for numerical solutions so as to overcome the problem that it is difficult to obtain the analytical solution to nonlinear problems. Due to the significant regional differences in ocean circulation in different sea areas, the response of a specific sea area or a specific ocean circulation to climate warming will be significantly different. Therefore, Wang and others effectively overcome the regional differences by integrating the large-scale marine kinetic energy in the whole global sea depth and using the integrated marine kinetic energy as an index to judge the changes in marine circulation [11]. Based on the monthly average wod13 temperature and salt data of climate state, this paper divides the water masses in the South China Sea by using the grey correlation cluster analysis method and analyzes the temperature and salt distribution characteristics and seasonal variation law of each water mass by combining the systematic cluster tree method and temperature and Salt Point aggregation map.

3. Research Methods

3.1. Data Preparation. The data used for analysis in this paper is the world ocean database2021 (wod21). The temperature and salt data in this database mainly include observation data such as high-resolution CTD, water temperature detector (MBT, XBT), drifting buoy (DRB), profile buoy (PFL), and anchored buoy (MRB) [12]. The time range of n in this paper is from January 2021 to March 2021 in $e-105^\circ$ space. The stations in each season can be distributed throughout the South China Sea.

When processing the data, only the sections with more than three temperature and salt data are retained. Because this paper only uses the temperature and salt data to cluster the water masses in the South China Sea, only the elements of longitude, latitude, time, depth, temperature, and salinity are retained in the data. After deleting the unqualified sections through quality control, there are 29317 sections in total. The seasonal distribution of the number of sections is shown in Figure 2, including 7105 in winter, 7378 in spring, 7445 in summer, and 7389 in autumn. The seasonal distribution is relatively uniform [13].

Since wod21 data is measured data with wide sources and a large time span, and the quality of data is uneven, in order to ensure that the data used for analysis can get more reasonable results, some processing needs to be carried out on the original data before specific research, and finally, 12-month monthly average data of climate state need to be obtained. The data processing process is as follows:

- (1) Delete the data whose salinity value is all NaN. Wod21 summarizes all the measured data. For some instruments (such as thermometers), the data obtained lack temperature or salinity data, and the salinity value is a very important element in water mass analysis, so these data are deleted.
- (2) Extract the required elements and unify the format. The longitude and latitude, depth, temperature, and salinity elements in the original data are extracted.

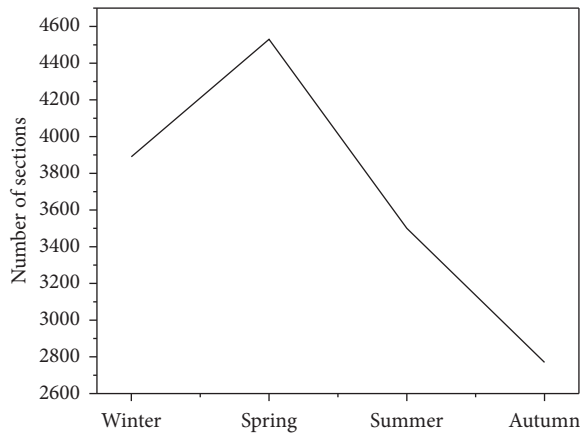


FIGURE 2: Distribution of section number.

The original format of time data is a string, which needs to be converted into an array of adult month day format. For data without time value, the time of adjacent data is taken [14].

- (3) Extract the data of the South China Sea and delete the obviously wrong values. The temperature range is 0–40. For salinity, the coastal water is greatly affected by river water and the salinity is low, forming a large difference from the salinity values of other sea areas in the South China Sea. Therefore, the salinity value less than 31 is assigned as 31.
- (4) Calculate the monthly average data of the climate state. Because the data are stored in years, and the site distribution is different every year. Therefore, when merging the data of the same month in different years, directly add the data with different site locations, and further compare the water depth with the data with the same site location. If the water depth is different, directly add the data, and if the water depth is the same, average the temperature and salt value.
- (5) Delete sites with less than three vertical values. Site data with less than three values in the vertical direction.
- (6) When used in clustering analysis, the data will be biased to the surface, resulting in the error of clustering results.
- (7) Moving to average the profile. When drawing salinity depth and temperature-depth curves on the profile, it is found that the measured data are often prone to “burrs”. Therefore, the sliding average of temperature and salinity is carried out, and the temperature and salt value corresponding to the original depth are taken.
- (8) Interpolate data to grid points. The data processed according to the above steps can be used for cluster analysis. However, the uneven distribution of sites may lead to clustering results biased towards areas with more data distribution. Therefore, the data are interpolated, with the horizontal interval of 0.1° and the vertical interval of 5 m.

The data processed by quality control basically conforms to the water characteristics of the South China Sea, but there will still be a small number of unqualified points, which will not affect the cluster analysis of water masses. However, in the clustering process, the step of eliminating unqualified points is added, hoping to get more reasonable results [15]. In addition, the previous water mass classification results are mostly based on temperature and salt elements. Therefore, in this paper, only two elements of temperature and salinity are selected in cluster analysis, which is convenient to compare and analyze the water mass classification results with the previous conclusions.

3.2. Grey System Theory. In the field of information, people usually use the depth of color to express the clarity of information. “Black” means the information is unknown, “white” means the information is known, “gray” means some information is unknown and some information is known. For this part of the information system represented by “gray”, we call it the “gray system”. Grey system theory mainly studies those poor information uncertain systems with “some information being known and some information unknown”. Through the analysis of the known part of the information, the possibility of the unknown part of the information is predicted, which is similar to semi-supervised learning. Grey correlation analysis and grey clustering are important branches of grey system theory. The grey correlation analysis method has no specific requirements for the sample size and regularity, and the amount of calculation is small, so there will be no inconsistency between the quantitative results and the qualitative analysis results. The grey relational clustering method simplifies the complexity of the system by merging similar factors [16].

In the traditional recommendation algorithm, the similarity of users or items is usually calculated according to the historical behavior data generated by users, then the similarity is sorted, and finally, recommended to users according to the sorting results. However, the historical behavior data of users are usually incomplete, heterogeneous, and loose. Such data will have a negative impact on the recommendation algorithm. The grey system theory has a good processing effect on these kind of data. Its advantages in processing data are very suitable for solving the problem of data sparsity in the recommendation system and can well alleviate the cold start problem.

3.2.1. Grey Relational Analysis Theory. Grey correlation mainly studies the uncertain correlation between various factors. Before grey correlation analysis, first find the mapping quantity that can reflect the behavior characteristics of the system, determine the effective factors affecting the system, and deal with them appropriately, then calculate the correlation coefficient and correlation degree between various factors, and finally analyze according to the calculation results [17]. In essence, this method judges the degree of correlation according to the similarity of the sequence curve of factors. The relevant definitions of grey correlation analysis theory are given below.

Define the mapping quantity of system behavior characteristics as the following formula:

$$X_i = (x_i(1), x_i(2), \dots, x_i(n)), i = 0, 1, 2, \dots, m. \quad (1)$$

Definition 2. Grey correlation degree: let x_0 be the mapping quantity of system characteristics and x_i be the mapping quantity of other relevant factors of the system.

$$\gamma(x_0(k), x_i(k)) = \frac{\min_i \min_k |x_0(k) - x_i(k)| + \zeta \max_i \max_k |x_0(k) - x_i(k)|}{|x_0(k) - x_i(k)| + \zeta \max_i \max_k |x_0(k) - x_i(k)|}, \quad (2)$$

where, $\gamma(x_0(k), x_i(k))$ represents the correlation coefficient between x_i and x_0 at point k , and ζ represents the resolution coefficient and $\zeta \in (0, 1)$.

$$\gamma(X_0, X_i) = \frac{1}{n} \sum_{k=1}^n \gamma(x_0(k), x_i(k)), \quad (3)$$

where, $\gamma(X_0, X_i)$ represents the grey correlation degree of x_i to x_0 , and formula (3) meets the following four characteristics:

- (1) Normative, indicating that any two system behavior mappings cannot be strictly unrelated.

$$0 < \gamma(X_0, X_i) \leq 1 \\ \gamma(X_0, X_i) = 1 \Leftrightarrow X_0 = X_i \quad (4)$$

- (2) Integrity, indicating that the environment has an impact on the grey correlation degree. For $bX_i, X_j \in X = \{X_s \mid s = 0, 1, 2, \dots, m; m \geq 2\}$, there

$$\gamma(X_i, X_j) \neq \gamma(X_j, X_i) (i \neq j). \quad (5)$$

- (3) Even pair symmetry shows that when there are only two mapping quantities of system behavior characteristics, the pairwise comparison meets the pairwise symmetry. For $X_i, X_j \in X$, there is the following formula:

$$\gamma(X_i, X_j) = \gamma(X_j, X_i) \Leftrightarrow X = \{X_i, X_j\}. \quad (6)$$

- (4) Proximity indicates that it restricts the quantification of grey correlation degree.

$$|x_0(k) - x_i(k)| \text{ smaller, } \gamma(x_0(k), x_i(k)) \text{ bigger}. \quad (7)$$

According to the above definition, the steps of calculating the grey correlation degree are as follows:

- (i) Step 1: find the initial value image of the behavior characteristic mapping quantity of each system, as shown in the following formula:

$$X'_i = \frac{X_i}{x_i}(1) = (x'_i(1), x'_i(2), \dots, x'_i(n)), \quad (8)$$

$$i = 0, 1, 2, \dots, m.$$

- (i) Step 2: calculate the difference mapping quantity, as shown in the following formula:

$$\Delta_i(k) = |x'_0(k) - x'_i(k)|, \\ \Delta_i = (\Delta_i(1), \Delta_i(2), \dots, \Delta_i(n)), \\ i = 0, 1, 2, \dots, m. \quad (9)$$

- (i) Step 3: find the maximum difference and minimum difference between the two poles, as shown in the following formula:

$$M = \max_i \max_k \Delta_i(k), \\ m = \min_i \min_k \Delta_i(k). \quad (10)$$

- (i) Step 4: calculate the grey correlation coefficient, as shown in the following formula:

$$\gamma_{0i}(k) = \frac{m + \zeta M}{\Delta_i(k) + \zeta M}, \zeta \in (0, 1), \quad (11)$$

$$k = i = 1, 2, \dots, n; i = 1, 2, \dots, m.$$

Step 5: calculate the grey correlation degree as follows:

$$\gamma_{0i} = \frac{1}{n} \sum_{k=1}^n \gamma_{0i}(k), i = 1, 2, \dots, m. \quad (12)$$

3.2.2. Grey Relational Clustering Theory. Grey correlation clustering is a method that obtains grey correlation matrix according to a grey correlation analysis and integrates some observation indexes or observation objects into several definable categories [18]. The calculation steps of grey correlation clustering are given below.

- (i) Step 1: determine the project characteristic data. There are n items, each item has m characteristic data, and all the data are as follows:

$$X_1 = (x_1(1), x_1(2), \dots, x_1(n)), \\ X_2 = (x_2(1), x_2(2), \dots, x_2(n)), \\ \dots \dots \dots \\ X_m = (x_m(1), x_m(2), \dots, x_m(n)). \quad (13)$$

Step 2: calculate the grey absolute correlation degree to obtain the grey correlation matrix. For all $i \leq j, i, j = 1, 2, \dots, m$, the grey absolute correlation degree E_{ij} of X_i and X_j is calculated in accordance with the following formula, and the grey correlation matrix A is obtained:

$$\varepsilon_{ij} = \frac{1 + |s_i| + |s_j|}{1 + |s_i| + |s_j| + |s_j - s_i|}, \quad (14)$$

where, $|s_i| = \int_1^n (X_i - x_i(1))dt, |s_j| = \int_1^n (X_j - x_j(1))dt$

$$A = \begin{bmatrix} \varepsilon_{11} & \varepsilon_{12} & \cdots & \varepsilon_{1m} \\ & \varepsilon_{22} & \cdots & \varepsilon_{2m} \\ & & \ddots & \vdots \\ & & & \varepsilon_{mm} \end{bmatrix}. \quad (15)$$

$\varepsilon_{ii} = 1; i = 1, 2, \dots, \text{min matrix.}$

Step 3: select appropriate parameters to cluster the characteristic variables.

The critical value $r \in [0, 1]$, generally $r > 0.5$. If $\varepsilon_{ij} \geq r (i \neq j)$, X_i and X_j are similar characteristics. In practical problems, the value of r can be changed according to needs. When $r \rightarrow 1$, the finer the classification, the fewer are the variables in each group. On the contrary, $r \rightarrow 0$, the coarser the classification, the more are the variables in each group.

3.3. T-S Point Aggregation Diagram. T-S point aggregation diagram has been used by many scholars for the analysis of water masses because of its simple method and strong intuition. In the existing analysis, water masses are mostly divided according to the density of scattered points on the T-S point aggregation diagram based on the relative uniformity of physical and chemical properties of water masses. However, the distribution of point sets on each map will change with the change in coordinate scale, resulting in different results due to the difference between people and the map [19]. In addition, the application of the T-S diagram to analyze shallow water masses has its limitations. It is only suitable for analyzing water masses with large differences in temperature and salinity.

Although the T-S point aggregation map cannot be directly used for water mass division, it can solve many other problems. For example, when the accuracy of the data is uncertain, the most reasonable results cannot be obtained by direct systematic clustering. The points with obvious observation errors can be eliminated according to the point clustering diagram before clustering. When the analysis results are not required to be very accurate, it can quickly give qualitative conclusions, which are essential basic materials for further quantitative calculation. In addition, for the mixing zone between water masses, the space occupied by it and the difference between the core properties of the two water masses mainly depends on whether there are points on the T-S point aggregation diagram, and each point represents a certain space. In this paper, by observing

whether the scattered points of each type in the T-S point aggregation diagram gather on the point aggregation diagram, we can detect whether the clustering result of the grey correlation clustering analysis is reasonable. According to the distribution of water masses with different properties on the point aggregation diagram, we can roughly obtain the temperature and salt properties of each water mass, so as to analyze the degree of water mass degeneration and the law of seasonal change.

4. Result Analysis

4.1. Water Mass Properties in Winter. In winter (January), the vertical distribution of the South China Seawater layer is obtained by using the grey correlation clustering method. From the sea surface down, it is surface water, subsurface water, sub-middle water, middle water, and deep water, which has an obvious layered structure. In the T-S point aggregation diagram, the temperature salt range of surface and subsurface seawater is large. After further horizontal division, the surface water is coastal flushing water, near-shore mixed water, South China Sea surface water, and Kuroshio surface water, and the subsurface water is divided into the South China Sea subsurface water and Kuroshio subsurface water, as shown in Table 1 below.

The deep water in the South China Sea is mainly distributed in the sea area deeper than 900 m, which is the deepest water mass in the distribution range. The temperature is lower than 5.0°C, the salinity range is 34.35–34.62, and its temperature and salt properties are basically consistent with the deep water in the Western Pacific [20].

4.2. Nature of Water Mass in Spring. Spring is the transitional season from winter to summer, and the properties of water masses are often between the two seasons. Obvious stratification still exists in each water mass. It is not difficult to find through the corresponding T-S point aggregation diagram that the temperature of water in each layer increases slightly compared with that in winter, as shown in Table 2 below.

In order to study the regional change process of the nature of each water mass, cluster analysis was carried out according to the division method of water mass in winter. In spring (April), the change law of Pacific surface water with high temperature and high salt entering the South China Sea is similar to that in winter, which gradually decreases or even disappears. Deep water in the South China Sea exists in the sea area more than 800 m deep, the temperature value is lower than 5.5°C, and the salinity range is 34.30–34.70.

4.3. Water Mass Properties in Summer. Each water mass still has an obvious stratification phenomenon. From the sea surface down, it is surface water, sub-surface water, sub-middle water, middle water, and deep water. Under the influence of thermal factors in summer, the sea surface heats up, and the atmosphere transports heat to the ocean. This heat can affect the depth of the whole South China Sea, resulting in the temperature of each water mass being higher

TABLE 1: Water mass properties in winter.

Arrangement	Depth	Bit density	Temperature	Salinity
Surface	0–100	20.5–23.7	21.5–29	32.70–34.70
Subsurface layer	100–200	23.7–25.5	15–21.5	34.00–34.90
Secondary middle	200–350	25.5–26.6	9.8–15	34.40–34.70
Middle level	350–900	26.5–27.2	4.5–10	34.25–34.50
Deep level	>900	27.2–27.7	2–5	34.35–34.62

TABLE 2: Water mass properties in spring.

Arrangement	Depth	Bit density	Temperature	Salinity
Surface	0–100	20.5–24.5	21–30.5	33.00–34.80
Subsurface layer	100–200	24.5–25.5	15.5–21	34.10–34.90
Secondary middle	200–300	25.5–26.3	11–15.8	34.30–34.70
Middle level	300–800	26.3–27.2	5.5–11	34.25–34.50
Deep level	>800	27–27.8	1.5–5.5	34.30–34.70

TABLE 3: Water mass properties in summer.

Arrangement	Depth	Bit density	Temperature	Salinity
Surface	0–120	20–24	22–30.5	32.50–34.65
Subsurface layer	120–200	23.5–25.5	16–22	34.00–34.85
Secondary middle	200–350	25.25–26.4	11–16	34.35–34.65
Middle level	350–800	26.3–27.2	5.5–11	34.25–34.50
Deep level	>800	27–27.8	1.5–5.5	34.30–34.70

TABLE 4: Water mass properties in autumn.

Arrangement	Depth	Bit density	Temperature	Salinity
Surface	0–100	20.5–24	21.5–29	32.60–34.80
Subsurface layer	100–200	24–25.4	16–21.5	34.00–34.85
Secondary middle	200–350	25.4–26.4	11–16	34.30–34.70
Middle level	350–850	26.4–27.2	5.8–11	34.20–34.45
Deep level	>850	27–27.8	2–5.8	34.30–34.80

than that in winter. However, due to the increase of precipitation in summer and the increase of runoff of continental rivers, the seawater is diluted and the salinity of seawater is reduced. Therefore, the salinity value of each water mass is slightly lower than that of the winter water mass. Through the analysis of the T-S point aggregation map, it is found that the mixing degree of South China Seawater and external seawater in surface water and subsurface water is low, which is far less than that in winter, as shown in Table 3 below.

There are two kinds of water bodies in the surface water. Under the action of the southwest monsoon in summer, the low salt water from the Java Sea mixes with the water in the Gulf of Thailand and enters the south of the South China Sea to form the continental shelf water in the south of South China Sea. Because the temperature and salt properties of the water mass are similar to the surface water of the South China Sea in summer, the two are not divided when clustering by temperature and salt values. Considering the different sources of water, the water in the southern continental shelf of the South China Sea is classified as an independent water mass, and the water mass only exists for

half a year of summer due to the influence of monsoon. The deep water in the South China Sea is distributed in the sea area with a depth of more than 800 m. The temperature value is lower than 5.5°C, and the salinity value is 34.30–34.70.

4.4. Nature of Water Mass in Autumn. Autumn is the intermediate period from summer to winter, and the temperature and salt properties of water masses are similar to those in spring. From the sea surface down, there are surface water, sub-surface water, sub-middle water, middle water, and deep water. In the T-S scatter diagram corresponding to each water layer, there are two kinds of water bodies with large differences in salinity sub-middle water, middle water, and deep water. The data of high salt water bodies are from 1985 and distributed in the central sea area of the South China Sea, and the specific causes of clustering are unknown, as shown in Table 4 below.

The clustering phenomenon of the lower water body of the South China Sea is often accompanied by the clustering of the upper water body, which indicates that this phenomenon is caused by different data years. In the surface and

TABLE 5: Properties of water masses in the South China Sea.

Name	Symbol	Source	Depth range/m	Temperature range/°C (early winter and late summer)	Salinity range (early winter and late summer)
Coastal freshwater mass	F	Continental runoff	<20		
Nearshore mixed water mass	M	The coastal fresh water is mixed with the external seawater to form	<75		
South China sea surface water mass	S	Western Pacific surface water	0–100 0–120		
Continental shelf water in the southern South China Sea (only in summer)	TS	Java Sea water and Gulf of Thailand water mixed to form	0–120		
Kuroshio surface water mass	KS	Kuroshio surface water	0–100		
Kuroshio subsurface water mass	KU	Kuroshio subsurface water	100–250		
South China Sea subsurface water mass	U	Western Pacific subsurface water	100–200 120–200	15.0–21.5 6.0–22.0	34.00–34.70 34.00–34.65
South China Sea sub-middle water mass	UI	Western Pacific subtropical thermocline water	200–350 200–350	9.8–15.0 11.0–16.0	34.40–34.70 34.35–34.65
Middle water mass in the South China Sea	I	Western Pacific middle water	350–900 350–800	4.5–10.0 5.5–11.0	34.40–34.50 34.39–34.55
Deep water mass in the South China Sea	D	Western Pacific deep water	>900 >800	<5.0 <5.5	34.35–34.62 34.30–34.70

subsurface water bodies, the mixed water between different water masses mainly comes from the sea area near the Luzon Strait. Due to the intense mixing of surface water and subsurface water, the surface water is further divided into coastal flushing fresh water, nearshore mixed water, South China Sea surface water, and Kuroshio surface water, and the subsurface water is further divided into Kuroshio subsurface water and South China Sea subsurface water. Deep water in the South China Sea is distributed in the sea area with a depth of 850 m, the temperature value is lower than 5.5 °C, and the salinity range is 34.30–34.80.

4.5. Seasonal Variation of Water Mass. In the vertical division, the South China Seawater mass is divided into five layers: surface water, subsurface water, sub-middle water, middle water, and deep water. Through the previous discussion, on the basis of vertical division, the surface water and subsurface water are further divided, and finally, the South China Sea is divided into 10 water masses: coastal alluvial fresh water, nearshore mixed water, Kuroshio surface water, Kuroshio subsurface water, South China Sea surface water, South China Sea shelf water (only in summer), South China Sea subsurface water, South China Sea sub-middle water, South China Sea middle water, and the South China Sea deep water. The deep water in the South China Sea is mainly distributed in the basin with a depth of 900m. The temperature value is lower than 5.5°C, and the salinity range is 34.30–34.70. The temperature and salt properties are basically consistent with the deep water in the Western Pacific. The seasonal and regional differences in temperature and salt properties of this water mass are not obvious. It is the most stable water mass in the South China Sea. The properties of each water mass are shown in Table 5 below.

By analyzing the properties of temperature and salt in each region, it is not difficult to find that the water masses in the South China Sea are formed after the Pacific water enters the South China Sea through the Luzon Strait. The surface and subsurface water are significantly affected and strongly denatured by the external seawater. The degree of denaturation of sub-middle, middle, and deep water masses is weak. After entering the South China Sea, the Kuroshio water is mainly distributed in the northwest of Luzon Strait. The invasion intensity is stronger in winter than in summer, and the sub-surface water of Kuroshio is stronger than the surface water of Kuroshio. The properties of the above water masses are basically consistent with the existing conclusions, but there are still a few differences, which need to be explained by the interannual variation law of water masses.

5. Conclusion

Based on the WOD13 temperature and salt observation data from 1966 to 2013, this paper uses the grey correlation clustering method to divide the water masses in the whole South China Sea and uses the system clustering method to support the division results. Combined with the T-S point clustering map of the whole region and sub-region of the South China sea, this paper analyzes the distribution, temperature and salt properties, and seasonal variation law of each water mass in the South China Sea. In the clustering process of water masses, this paper creatively uses the intraclass distance sum function and density value function to determine the “number of water masses” and “initial center” respectively, which improves the efficiency and accuracy of operation. Through the grey correlation clustering method, the water mass in the South China Sea is vertically divided into five layers, namely surface water, subsurface water, sub-middle water, middle water, and deep

water. Due to the large differences in temperature and salinity between different water layers, when using the clustering method in the whole sea area of the South China Sea, it cannot distinguish the specific different water masses in each layer of water, especially the surface water and subsurface water. In the T-S point clustering diagram, the temperature and salt points are relatively dispersed and obviously contain a variety of independent water masses. There is a close relationship between ocean circulation and water mass. The former is the motion carrier of the latter, and the latter is the motion result of the former. Therefore, the South China Sea circulation has an important impact on the generation and dissipation process of the South China Sea water mass, and the distribution and hydrological characteristics of the water mass can indirectly reflect the South China Sea circulation path on various scales. In future research, we can analyze the relationship between the seasonal and interannual changes of the South China Sea water mass and the South China Sea circulation and Kuroshio in combination with reanalysis and model data.

Data Availability

The data used to support the findings of this study are available from the corresponding author upon request.

Conflicts of Interest

The authors declare that they have no conflicts of interest.

References

- [1] M. A. Sorokin, P. S. Petrov, D. D. Kaplunenko, A. A. Golov, and Y. N. Morgunov, "Predicting effective propagation velocities of acoustic signals using an ocean circulation model," *Acoustical Physics*, vol. 67, no. 5, pp. 501–511, 2021.
- [2] R. Huang, P. Yan, and X. Yang, "Knowledge map visualization of technology hotspots and development trends in China's textile manufacturing industry," *IET Collaborative Intelligent Manufacturing*, vol. 3, no. 3, pp. 243–251, 2021.
- [3] W. G. Cheon and J. S. Kug, "The role of oscillating southern hemisphere westerly winds: global ocean circulation," *Journal of Climate*, vol. 33, no. 6, pp. 2111–2130, 2020.
- [4] F. B. Dias, R. Fiedler, S. J. Marsland et al., "Ocean heat storage in response to changing ocean circulation processes," *Journal of Climate*, vol. 33, no. 21, pp. 9065–9082, 2020.
- [5] J. Scheen and T. F. Stocker, "Effect of changing ocean circulation on deep ocean temperature in the last millennium," *Earth System Dynamics*, vol. 11, no. 4, pp. 925–951, 2020.
- [6] X. Liu, J. Liu, J. Chen, F. Zhong, and C. Ma, "Study on treatment of printing and dyeing waste gas in the atmosphere with Ce-Mn/GF catalyst," *Arabian Journal of Geosciences*, vol. 14, no. 8, pp. 737–6.
- [7] M. S. Pradeep Raj, P. Manimegalai, P. Ajay, and J. Amose, "Lipid data acquisition for devices treatment of coronary diseases health stuff on the internet of medical things," *Journal of Physics: Conference Series*, vol. 1937, no. 1, Article ID 012038, 2021.
- [8] C. Hao, L. Song, and W. Zhao, "Hysplit-based demarcation of regions affected by water vapors from the south China sea and the bay of bengal," *European Journal of Remote Sensing*, vol. 54, pp. 348–355, 2020.
- [9] A. L. Sobisevich, E. I. Suetnova, and R. A. Zhostkov, "Influence of layered structures of the seabed on the formation of gas hydrates in the area surrounding deep-sea mud volcanoes: a mathematical model," *Doklady Earth Sciences*, vol. 503, no. 1, pp. 100–103, 2022.
- [10] X. Zhao, D. Wang, H. Xu et al., "Water deep mapping from hj-1b satellite data by a deep network model in the sea area of pearl river estuary, China," *Open Geosciences*, vol. 13, no. 1, pp. 782–795, 2021.
- [11] X. Wang and Y. Mu, "Research on grey relational clustering model of multiobjective human resources based on time constraint," *Scientific Programming*, vol. 2021, no. 8, pp. 1–9, 2021.
- [12] F. Gao, C. Hei, J. Liu, Y. Li, and L. Shui, "Synthetic positioning error modelling of a feed axis for a precision p machine tool," *International Journal of Advanced Manufacturing Technology*, vol. 114, no. 5–6, pp. 1385–1394, 2021.
- [13] R. Kumar, V. Jain, N. Chauhan, and N. Chand, "An adaptive prediction strategy with clustering in wireless sensor network," *International Journal of Wireless Information Networks*, vol. 27, no. 4, pp. 575–587, 2020.
- [14] S. A. Ganiyu, K. S. Are, and O. T. Olurin, "Assessment of geotechnical and physico-chemical properties of age-long greywater-contaminated soils in basement complex areas, southwest Nigeria," *Applied Water Science*, vol. 10, no. 5, pp. 114–115, 2020.
- [15] M. E. O. Firat, "Experimental investigation on the thermal characteristics and grey correlation analysis of frost penetration depths for different subgrade soils," *Environmental Earth Sciences*, vol. 80, no. 11, pp. 394–412, 2021.
- [16] J. H. Kim, B. H. Choi, H. R. Kim, C. T. Rim, and Y. S. Kim, "Single-variable-input active sidelobe suppression method for synthesized magnetic field focusing technology and its optimization," *IEEE Transactions on Industrial Electronics*, vol. 67, no. 11, pp. 9813–9823, 2020.
- [17] T. Aryeni, Q. Deng, and V. Ginting, "On the application of generalized finite element method for quasilinear elliptic two-point bvp," *Journal of Scientific Computing*, vol. 90, no. 1, pp. 33–38, 2022.
- [18] A. Sharma, G. Rathee, R. Kumar et al., "A secure, energy- and sla-efficient (sese) e-healthcare framework for quickest data transmission using cyber-physical system," *Sensors*, vol. 19, no. 9, p. 2119, 2019.
- [19] P. Ataei Delshad and T. Lotfi, "On the local convergence of kung-traub's two-point method and its dynamics," *Applications of Mathematics*, vol. 65, no. 4, pp. 379–406, 2020.
- [20] Z. Guo and Z. Xiao, "Research on online calibration of lidar and camera for intelligent connected vehicles based on depth-edge matching," *Nonlinear Engineering*, vol. 10, no. 1, pp. 469–476, 2021.